Transaction B: Mechanical Engineering
Vol. 16, No. 3, pp. 248–252

SCIENTIA IRANICA

Characterization of Sputtered NiTi Shape Memory Alloy Thin Films

S. Sanjabi[1,*], M. Naderi[1], H. Zare Bidaki[1] and S.K. Sadrnezhaad[2]

Abstract. *During recent years, many investigations have been carried out to determine how to select different materials for the making of Micro Electro Mechanical Systems (MEMS) and bio-MEMS. The NiTi shape memory alloy thin film has been much regarded as a promising candidate for MEMS due to its unique shape memory effect and high energy output. In this research, NiTi thin film was fabricated using a sputtering technique from separate elemental Ni and Ti targets. The characterizations of the deposited films were investigated using different analysis techniques, such as Field Emission SEM, DSC, XRD, electrical resistivity measurement and nanoindentation.*

Keywords: *NiTi thin film; Sputtering; Characterization; Shape memory effect.*

INTRODUCTION

Shape memory is the unique property of some alloys, which returns to its original shape with heating. Shape-Memory Alloys (SMAs) possess an array of desirable properties: High power to weight (or force to volume) ratio (thus having the ability to recover large transformation stresses and strains upon heating and cooling), peudoelasticity (or superelasticity); a high damping capacity and good chemical resistance and biocompatibility [1,2]. More recently, thin film SMA has been recognized as a promising and high performance material in the field of Micro-Electro-Mechanical Systems (MEMS) since it can be patterned with standard lithography techniques and fabricated in a batch process [3].

Thin film SMA has only a small amount of thermal mass to heat or cool, thus the cycle (response) time can be reduced substantially and the speed of operation may be increased significantly. The application of SMA films in MEMS also facilitates the simplification of mechanisms with a flexibility of design and the creation of clean, friction free and non-vibration movements. MEMS-based micropumps and microvalves are attractive for many applications, such as implantable drug delivery, chemical analysis and analytical instruments etc. [4]. There are different designs for TiNi film based micropumps or microvalves and most of them use TiNi. Membrane grasping and manipulating small or micro-objects with high accuracy is required for a wide range of important applications, such as the assembly in microsystems, endoscopes for microsurgery and drug injection micro-manipulators for cells.

NiTi alloys are sensitive to the composition ratio of Ti and Ni: only 1% variation of composition can cause a 100°C shift in transformation temperatures [5]. From a practical point of view, only sputter deposition has succeeded so far and a perfect shape memory effect similar to bulk materials can be obtained [6].

In sputtering, an alloy target is generally used and the compositions of the sputtered films are always Ni-rich in comparison with the target (the films are Ti poor with respect to the target (by 2-4at%)), because the sputtering yield for Ni is higher than Ti [7]. The simplest and most common solution to this problem is to place small pieces of pure Ti onto the target to achieve the correct film stochiometry [8]. Composition adjustment using Ti (or Ni) plates requires the control of numerous parameters, such as number, geometry, size and position, and any subsequent change of the deposition parameters will require re-adjustment. This technique leads to high impurity levels, due to the large surface contribution.

1. *Department of Materials Science and Engineering, Tarbiat Modares University, Tehran, P.O. Box: 14115-143, Iran.*
2. *Department of Materials Science and Engineering, Sharif University of Technology, Tehran, P.O. Box 11155-9466, Iran.*
*. *Corresponding author. E-mail: sanjabi@modares.ac.ir*

Received 12 May 2007; received in revised form 26 February 2008; accepted 27 May 2008

The control of the film composition from separate targets controlled by the power ratio is more flexible and can overcome these problems. The control of composition uniformity is important, requiring appropriate deposition geometry (e.g. inclining the axes of the targets [9], optimizing the substrate-target distance and the size and shape of targets). In this study, shape memory NiTi films were fabricated by a simultaneous sputter deposition from separate elemental Ni and Ti targets (the mixing of elements before arrival at the substrate) and annealing at a relatively low temperature. The deposited films were characterized with respect to structure, transformation temperature and mechanical property.

EXPERIMENT DETAILS

Films were deposited by ultra high vacuum DC magnetron sputtering onto an unheated Si (1 0 0) substrate of dimension 10 mm × 5 mm. The deposition system allowed two magnetrons (target size: 35 mm × 55 mm), plus associated heater leads, instrumentation feedthroughs, viewing port and rotary shaft, to be placed on one standard 200 mm O.D. flange, inserted into a 150 mm I.D. nitrogen-cooled can. A constant flow of Ar (99.999%) was controlled with a leak valve during film deposition and different sputtering gas pressures were achieved by throttling the gate valve. The thickness of the film was measured by surface profilometry (Talysurf 6, Taylor-Hobson) using the step height on a masked silicon substrate: the deposition rate was calculated to be about 1 Am/h and the thickness of the films was around 2 μm.

as-deposited films were annealed at 500°C for 1 h in a vacuum furnace (base pressure $< 10^{-5}$ Pa) with heating and cooling rates of approximately 50°C/min. The composition of as-deposited films was determined by energy dispersive X-ray spectroscopy, using a JEOL JSM-5800LV operating at 15 keV. Films were examined by observing fracture cross-sections in a Field Emission Scanning Electron Microscope (FESEM) using a JEOL JSM-6340F. A Siemens D500, with a Cu-Kα(λ = 1.54056 A°) X-ray source at 40 kV and 40 mA was used for XRD as a function of temperature, and DSC (Q1000, TA instruments with the minimum required mass = 0.5 mg) was used to indicate the transformation temperatures at heating and cooling rates of 10°C/min. A standard four-point electrical resistivity measurement also characterized the transformation temperatures. Nanoindentation was performed using a Nanotest 600 (Micro-Materials Ltd., UK). A diamond indenter (tip radius of 10 micron) was used for spherical indentation, loading and unloading at 0.1 mN/s, giving indentation depths ranging from 20 to 500 nm. Both load and displacement were recorded during the entire loading and unloading cycle.

RESULTS AND DISCUSSION

Without substrate rotation, suitable powers were applied to each target to give similar deposition rates (of Ni and Ti) at the center of the substrate support. Figure 1 shows the resulting composition variation across the substrate support (the power ratio of Ti to Ni was around 3). The composition uniformity was affected by the deposition geometry. For example, a small deviation of the substrate holder from the horizontal plane led to around 1% variation across the 100 mm substrate holder diameter (0.01%/mm).

Important parameters which affect the quality of the films are target power (and hence the deposition rate), Ar gas pressure, substrate-target distance, substrate temperature, purity of material targets and the deposition environment. The Ar pressure and the target-substrate distance affect the energies of the depositing species, and thus film density, structural integrity and stress. At high Ar pressures, films often show low density containing structural defects, while at low pressures the structure is denser with fewer defects [10]. Films spanning a range of compositions, prepared at high Ar pressures (> 1 Pa), had a brittle structure and cracks were observed on the film surface; Figure 2a shows the extensive delamination at the NiTi/Si interface and cracks caused by in-plane, biaxial tensile stresses. Films covering a similar range of composition, prepared at low Ar pressures, exhibited a smooth, featureless surface structure; Figure 2b shows the cross-section of a film deposited at 0.6 Pa.

XRD of as-deposited films showed only a broad peak around 2θ = 42° and no crystalline peaks, suggesting an amorphous structure (see Figure 3). After annealing, in spite of similar composition, films deposited at two different gas pressures showed very different film structures. The XRD spectrum of a 51.2% Ti and film deposited at 1.2 Pa (see Figure 3a),

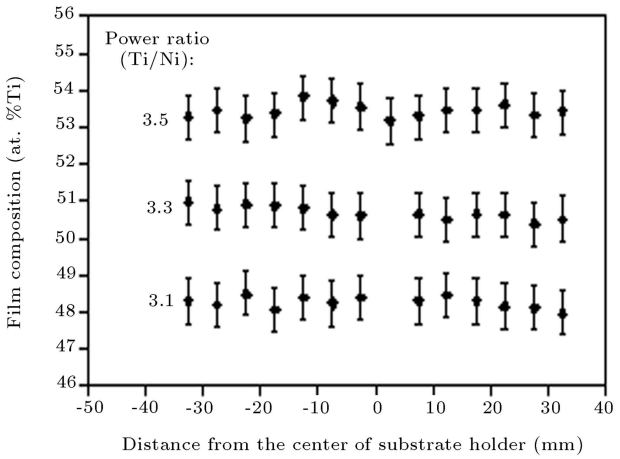

Figure 1. The composition variation across the substrate holder.

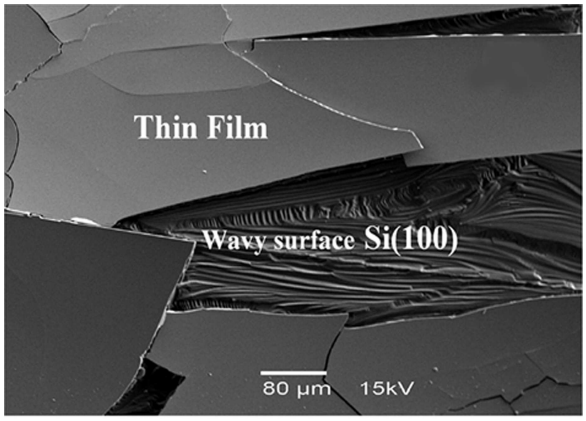

(a)

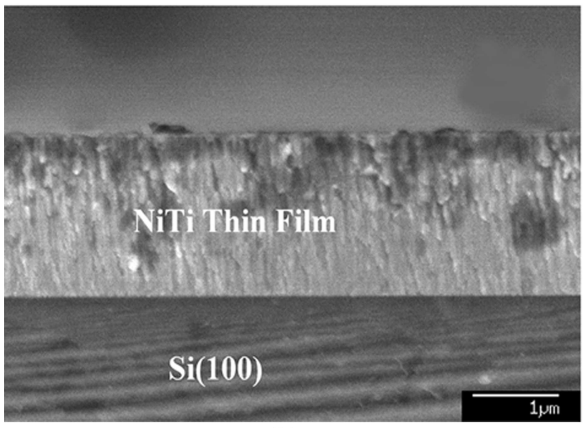

(b)

Figure 2. Scanning electron micrographs of films deposited at different Ar gas pressures: (a) plan view of a film deposited at 1.2 Pa, showing severe surface delamination, and (b) FESEM cross-section of a film deposited at 0.6 Pa.

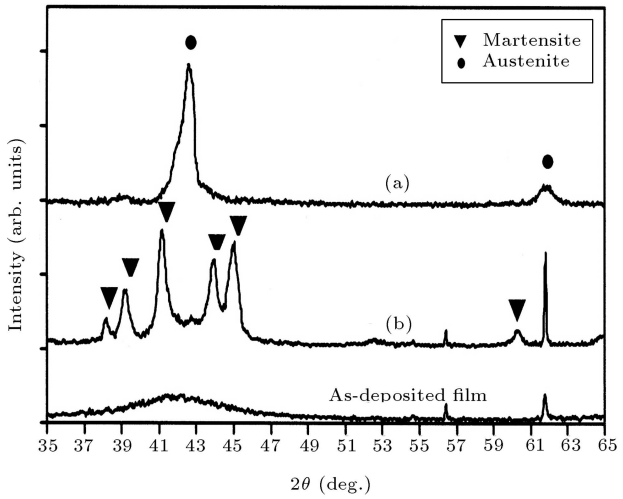

Figure 3. Room temperature XRD profiles of films deposited at different Argon pressures (annealed at 500°C): (a) 1.2 Pa with composition of $Ti_{51.2}Ni_{48.8}$ and (b) 0.6 Pa with composition of $Ti_{50.6}Ni_{49.4}$. XRD of an as-deposited film is also shown.

showed only an austenite phase (peaks at 42.7°and 62°, corresponding to 110 and 200 austenite reflections) at room temperature.

The shape memory effect of this film was characterized by electrical resistivity, as a function of temperature (see Figure 4a), confirming that the transformation temperature of this film is below room temperature. The loop of the shape memory during cooling and heating is not clear and one peak can be observed around 40°C. Following the deposition of a similar film composition at lower Ar pressure (0.6 Pa), the annealed film showed martensite peaks at room temperature. The existence of the martensite peaks at room temperature indicates that the shape memory effect and phase transformation occur above room temperature, as confirmed by the electrical resistivity measurement shown in Figure 4b.

These results illustrate that in spite of controlling the film composition, a poor shape memory effect can be obtained.

Thin films with different compositions were fabricated at the Ar gas pressure of 0.6 Pa and then

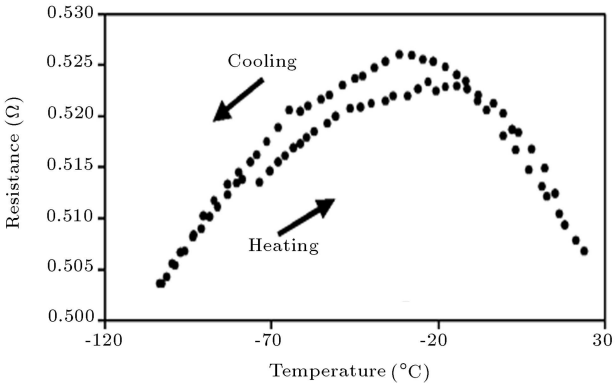

(a)

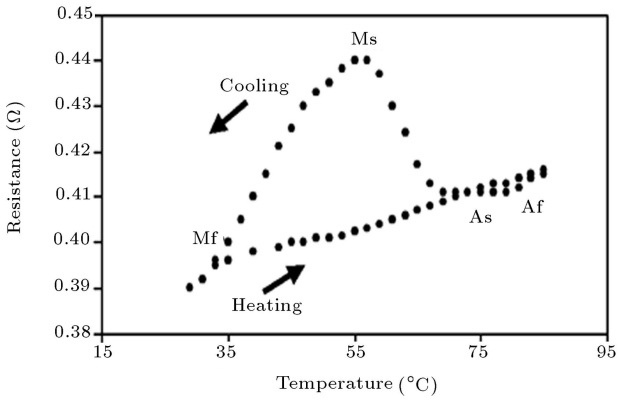

(b)

Figure 4. Electrical resistivity measurement as a function of temperature for films deposited at different Ar gas pressures and annealed at 500°C: (a) 1.2 Pa with composition of $Ti_{51.2}Ni_{48.8}$ and (b) 0.6 Pa with composition of $Ti_{50.6}Ni_{49.4}$.

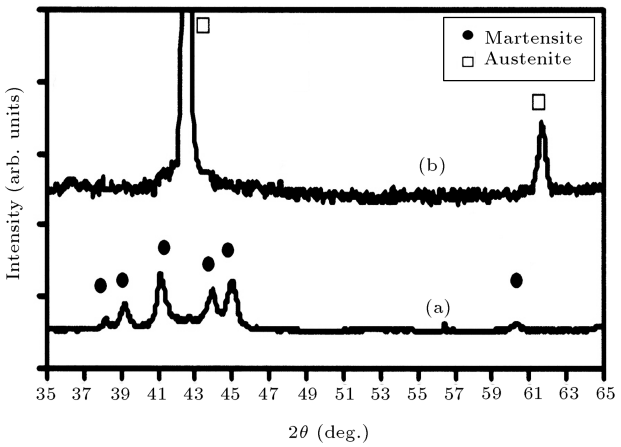

Figure 5. XRD trace of near-equiatomic ($Ti_{50.6}Ni_{49.4}$) (a) room temperature, and (b) 100°C (see text for indexing of peaks).

annealed at 500°C for 1 h. Figure 5 shows the XRD traces of annealed near equiatomic films at room temperature and 100°C. For an equiatomic NiTi film at room temperature, diffraction patterns showed peaks at 2θ = (38.2°, 39.1°, 41.3°, 44.05°, 45.1°, 60.2°) indexed respectively as 110, 002, 111, 020, 012 and 022 planes of the B19′ (monoclinic) martensite structure (Figure 5a). During heating to 100°C, the martensite peaks gradually disappeared and were replaced by a sharp peak at 2θ = 42.7°and a minor peak at 2θ = 62°(Figure 5b) which corresponds to austenite 110 and 200.

Annealed NiTi thin films undergo a martensitic phase transformation when cooled below their transformation temperature. The transformation temperatures of near equiatomic and Ti-rich films are above room temperature, while that of the Ni-rich film is lower. In Figure 6, which shows the DSC results of the near equiatomic NiTi film, a one-stage transformation is observed during heating, corresponding to B19′ to B2 transformation. The transformation enthalpy of 22.3 J/g confirms that this peak is related to a direct transformation from martensite to austenite phases; the transformation starts from 71°C and finishes at 86°C. During cooling, a two-stage transformation is observed, corresponding to a transformation between B2, R-phase and B19' phases. The austenite phase starts to transform to R-phase at around 60°C. The R-phase starts to change to the martensite phase at a temperature around 50°C and finishes at 30°C. This evaluation indicates that the martensite structure is dominant at room temperature and austenite at higher temperature (around 100°C) as indicated by XRD (Figure 5).

Figure 7 shows the indenter load versus the indentation depth as a function of the film composition (all indentation tests were conducted at room temperature). For the Ni-rich film, high elastic recovery was seen in the unloading curve, indicating the predominance of elastic or psuedo-elastic deformation. For near-equiatomic (Figure 7) there is much less evidence of such elastic recovery in the unloading curve, indicating predominantly plastic deformation. Interpreting the indentation response is a complex task due to dependence on the test temperature, strain level, applied stress and type of indenter. Recent reports suggest that a spherical indenter is optimum for understanding the shape memory effect and pseudo-elasticity. Our other measurements show that both Ti-rich and near-equiatomic films have the martensite structure at room temperature, while the Ni-rich film is austenitic. The mechanism of deformation under indentation has been discussed for both martensite and austenite bulk material structures; for austenite structures, both martensite formation and detwinning can

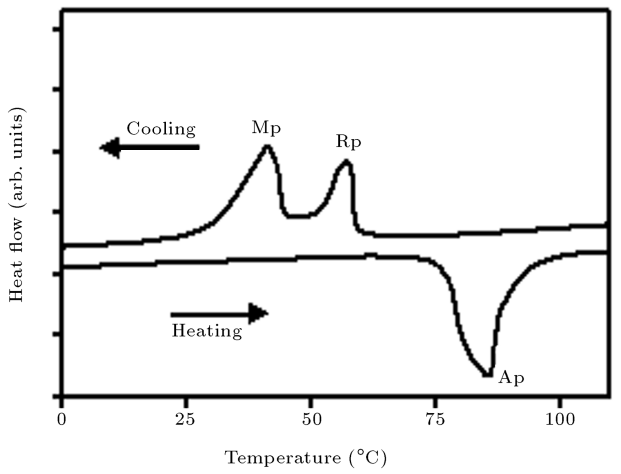

Figure 6. DSC trace of near-equiatomic ($Ti_{50.6}Ni_{49.4}$).

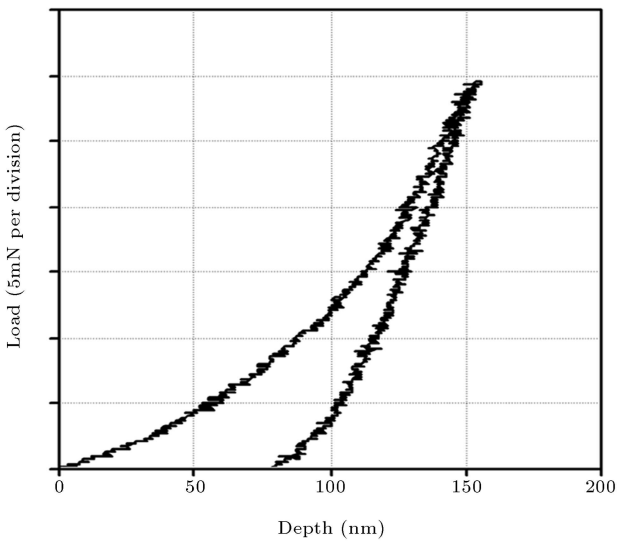

Figure 7. Load vs. displacement curve for near-equiatomic ($Ti_{50.6}Ni_{49.4}$).

occur, while in the martensitic phase only detwinning takes place. Martensite formation in the austenitic phase is metastable, and thus reverses on unloading, leading to recoverable strain, while detwinning results in permanent deformation unless a subsequent heating step is included.

CONCLUSIONS

The fabrication of shape memory TiNi thin films using simultaneous sputter deposition from separate elemental targets was demonstrated. The influence of the sputtering parameters on the quality of the film and shape memory effect has been illustrated; in spite of composition control, at higher Ar gas pressure the transformation temperature can occur below room temperature and the shape memory hysteresis loop during heating and cooling is not clear. Following deposition at low gas pressure, phase transformations showed a qualitatively similar behavior as a function of film composition to Ni-Ti bulk materials. Simultaneous sputter deposition from two targets offers flexibility in control of the required composition and it is simple to add another target for the fabrication of ternary shape memory thin films. Successful implementation of TiNi micro-actuators requires a good understanding of the relationship between the processing, microstructure and properties of TiNi films.

REFERENCES

1. Otsuka, K. and Ren, X. "Recent developments in the research of shape-memory alloys", *Intermetallics*, **7**, pp. 511-528 (1999).
2. Humbeeck, J.V. "Non-medical applications of shape-memory alloys", *Mater. Sci. Eng. A273-A275*, pp. 134-148 (1999).
3. Krulevitch, P., Lee, A.P., Ramsey, P.B., Trevino, J.C., Hamilton, J. and Northrup, M.A.M.A. "Thin film shape-memory alloy micro-actuators", *J. MEMS*, **5**, pp. 270-282 (1996).
4. Reynaerts, D., Peirs, J. and Van Brussel, H. "An implantable drug-delivery system based on shape memory alloy micro-actuation", *Sensors & Actuators A*, **61**, pp. 455-462 (1997).
5. Ikuta, K., Fujishiro, H., Hayashi, M. and Matsuura, T. "Laser ablation of Ni-Ti shape memory alloy thin film", *Proceedings of the First International Conference on Shape Memory and Superelastic Technologies*, Asilomar Conference Center, Pacific Grove, California, USA, p. 13 (1994).
6. Miyazaki, S. and Ishida, A. "Martensitic transformation and shape memory behavior in sputter-deposited TiNi-base thin films", *Mater. Sci. Eng., A Struct. Mater.: Prop. Microstruct. Process.*, **106**, pp. 273-275 (1999).
7. Grummon, D.S., Hou, L., Zhao, Z. and Pence, T.J. "Progress on sputter-deposited thermotractive titanium-nickel films", *J. de. Phys. IV*, **5**, p. 665 (1995).
8. Yamamoto, T. and Miyazaki, S. "Fabrication of TiNi-based shape memory alloy thin films by simultaneous multi-target sputtering method", *J. de Phys. IV*, **112**, p. 869 (2003).
9. Ishida, A., Takei, A. and Miyazaki, S. "Shape memory thin film of Ti-Ni formed by sputtering", *Thin Solid Films*, **228**, p. 210 (1993).
10. Thornton, J.A. "The microstructure of sputter-deposited coatings", *J. Vac. Sci. Technol., A, Vac. Surf. Films*, **4**(6), p. 3059 (1986).